Proceedings of ASME Turbo Expo 2011
GT2011
June 6-10, 2011, Vancouver, British Columbia, Canada

GT2011-46148

NUMERICAL MEANLINE ANALYSIS AND OVERALL PERFORMANCE PREDICTION OF RADIAL-INFLOW TURBINE FOR A 600 kW CYCLE GAS ENGINE.

Rubén A. Miranda Carrillo, Marco A. R. Nascimento
Universidade Federal de Itajubá – UNIFEI
Grupo de Estudos em Tecnologias em Conversão de Energia - GETEC
Instituto de Engenharia Mecânica
37500-903 Itajubá MG, Brasil.
55-35-3629 1355, e-mail: ruben.miranda@unifei.edu.br

ABSTRACT.

Radial-inflow turbines have been developed as one important power generation systems for distributed generation options, because they have demonstrated higher levels of efficiency than small axial flow turbine [1]. Radial-inflow turbine is a key part of microturbines and its aerodynamic performance affects directly on characteristics of whole microturbine system [2].

This paper presents the numerical meanline analysis and overall performance prediction of radial-inflow turbine for a 600 kW cycle gas engine using a One-dimensional Computer FORTRAN Code (OFC) [3]. This program was based mainly in non-dimensional parameters and it uses a one-dimensional solution of flow conditions through the turbine along the meanline. Comparison of predicted with analytical results determined performance for this turbine showed good agreement.

INTRODUCTION.

An aerodynamics performance analysis is essential for nearly all aspects of radial-inflow turbine aerodynamic design and application. One-dimensional computer programs and computational simulations are a promising means for the cost relief; however, they require a flexible software simulation system capable of integrating advanced multidisciplinary and multifidelity analysis methods. For this reason, the Federal University of Itajubá and its Energy Conversion Technology Research Group (GETEC), has worked on the development of projects focusing on the design of power units with varied fuel types. The aim has been to offer technical, economical and environmental solution to the problem of providing reliable and stable energy to the industrial segment and remote rural communities far from the interconnected electricity grid.

This paper presents the numerical meanline analysis and overall performance prediction of the nozzle and radial-inflow rotor for a 600 kW cycle gas turbine engine using a one-dimensional computer FORTRAN code (OFC), based mainly on non-dimensional parameters aimed at computational and work time reduction. The OFC results were compared with computer program for design and off-design analysis of radial-inflow turbines and analytical results taken from specialized literature. The comparisons showed the results were in agreement.

NOMENCLATURE.

A_{eff}	Effective area [m^3]
A_{geo}	Geometric area [m^3]
b	Blade or vane height [mm]
C	Absolute velocity [m/s]
CFD	Computational Fluid Dynamics
D	Diameter [mm]
$\dot{m}$	Mass flow rate [kg/s]
k	Polytropic constant
p_x	Static pressure [kPa]
P_{xx}	Total pressure [kPa]
P_{oo}	Inlet turbine total pressure [kPa]
Q	Volume flow rate at exit [m^3/s]
r	Radius [mm]

t	Thickness [mm]
T_x	Static temperature [K]
T_{xx}	Total temperature [K]
T_{oo}	Inlet turbine total temperature [K]
U	Blade speed [m/s]
$\dot{w}$	Specific work output [J/kg]
$\dot{w}_S$	Isentropic work output [J/kg]
Z_B	Number of blades o vanes

Greek Symbols

α	Absolute flow angle [°]
β	Relative flow angle [°]
η	Efficiency [%]
ω	Rotational speed [rad/s]
υ	Exit hub to shroud radius ratio
Δ	Radius variation [mm]

Subscripts

m	Mean
n	Nozzle
p	Polytropic
r	Rotor
ts	Total to static
tt	Total to total
0	Nozzle inlet
1	Nozzle outlet
2	Rotor inlet
3	Rotor outlet

A MEANLINE DESIGN POINT AND OFF-DESIGN METHOD.

The preliminary design of a radial turbine begins with the design specification, which could include requirements for shaft speed, power output, mass flow rate and turbine pressure ratio [4]. The OFC for the design and analysis of radial inflow turbine components uses a one-dimensional solution of flow conditions through the turbine along the meanline and includes consideration of nozzle and rotor trailing-edge blockage.

Figure 1 shows the surface analysis and includes consideration of nozzle and rotor trailing-edge blockage.

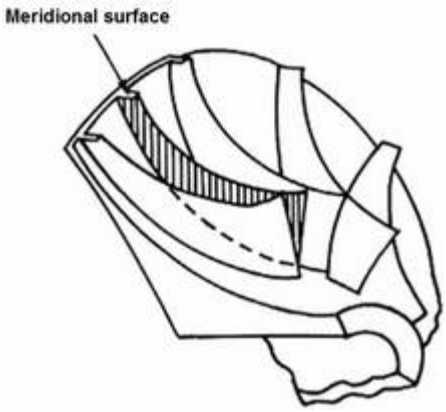

FIGURE 1. THE SURFACE OF ANALYSIS.

The blockage (B) refers to the difference between the real area that circulates the fluid and the geometric area of the component.

$$B = 1 - \frac{A_{eff}}{A_{geo}} \qquad 1)$$

The Figure 2 shows the effect of the blockage factor. The blockage refers to the difference between the real area that circulates the fluid and the geometric area of the component.

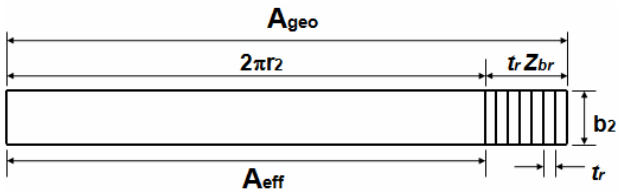

FIGURE 2. THE BLOCKAGE FACTOR.

The Figure 3 shows the meanline method. This analysis is based on the assumption that there is a mean streamline running through the machine and the conditions on this streamline are representative of the stations being considered [5]. The objective of a meanline analysis is to not reveal the full details of the flow state and velocity through the machine, but conversely, it is limited to determine the machine's overall performance or the combination of overall geometric parameters achieving maximum efficiency [6].

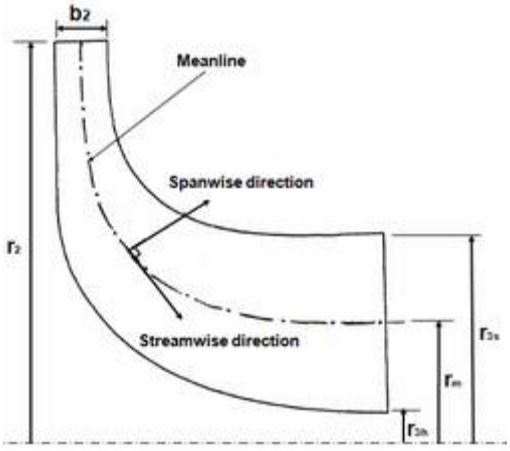

FIGURE 3. THE MEANLINE METHOD.

This work is compared with NASA TN D-8164 [7]. The main differences between the NASA computer program for the design analysis of radial inflow turbines and the one-dimensional computer FORTRAN code (OFC) consist of the quantity of the program input parameters utilized in the components preliminary design and the calculus methodology.

Perfect gas relations were used throughout. For any fixed speed, the velocity ratio V/V_{cr} at the radial-inflow rotor and nozzle exit is varied by uniform increments and for each increment, complete calculations are made at each station.

There are two main differences in the analytical procedure. First, the nozzle configuration, involved a blockage at the nozzle exit and large radial clearance between the nozzle and radial-inflow rotor. This is the station where the flow from the nozzle is assumed to occupy the entire cylindrical flow area.

The second difference is a change in radius from the rotor inlet to the rotor exit. This causes a change in the total temperature, relative to the rotor, and results in a modification in the expression for the pressure loss ratio across the rotor.

Table 1 shows that the OFC program utilizes 57% of input parameters while the NASA TN D-8164 utilizes 70%, also, knowledge of the turbine geometry and the basic overall dimension is required for the preliminary design.

TABLE 1. COMPARISON OF DESIGN POINT INPUT PARAMETERS.

Description	NASA TN D-8164	OFC
Mass flow rate	✓	--
Inlet turbine total temperature	✓	✓
Inlet turbine total pressure	✓	✓
Total to static turbine pressure ratio	--	✓
Total to static rotor efficiency	--	✓
Total nozzle efficiency	--	✓
Rotor inlet relative flow angle	--	✓
Rotor outlet relative flow angle	--	✓
Nozzle inlet absolute flow angle	✓	--
Nozzle outlet absolute flow angle	✓	--
Rotor exit hub to shroud radius ratio	✓	✓
Rotor exit shroud to rotor inlet radius ratio	✓	--
Nozzle inlet to rotor inlet radius ratio	✓	--
Nozzle exit to rotor inlet radius ratio	✓	--
Nozzle aspect ratio	✓	✓
Specific heat ratio	✓	✓
Tip clearance	✓	✓
Relative velocity ratio	--	✓
Rotor blade thickness	--	✓
Nozzle vane thickness	--	✓
Nozzle radius ratio	✓	✓
Rotor loss-coefficient	✓	--
Nozzle loss-coefficient	✓	--
Gas constant	✓	--
Rotative speed	✓	--
Shaft power	✓	--

NOZZLE AEROTHERMODYNAMIC DESIGN.

The nozzle consists of 17 vanes with a radial-flow inlet from a low Mach number. The design inlet and the exit angle is 54.59° and 77.97°, respectively. Both the trailing-edge and the leading-edge thickness are constant and the blockage factor is 0.98. Figure 4 shows the nozzle vane configuration.

FIGURE 4. NOZZLE VANE CONFIGURATION.

Table 2 presents the nozzle geometric and thermodynamic output parameters at the design point calculate by OFC.

TABLE 2. NOZZLE AEROTHERMODYNAMICS OUTPUTS.

Description	Inlet ($_0$) Values	Outlet ($_1$) Values	Units
Vane height	33.51	33.51	mm
Nozzle radius	278.48	227.67	mm
Thickness	1	1	mm
Number of vanes	17		--
Absolute flow angle	54.59	77.97	°
Ratio of nozzle inlet to rotor inlet diameter	1.25	--	--
Ratio of nozzle exit to rotor inlet diameter	--	1.04	--
Ratio of nozzle inlet vane height to rotor inlet diameter	0.07	--	--
Ratio of nozzle exit vane height to rotor inlet diameter	--	0.07	--
Ratio to nozzle inlet to nozzle exit diameter	1.19		--
Total temperature	1123	1123	K
Static temperature	1117.05	981.95	K
Total pressure	396	374.31	kPa
Static pressure	388.70	234.00	kPa
Absolute velocity	109.30	532.30	m/s

RADIAL-INFLOW ROTOR AEROTHERMODYNAMIC DESIGN.

The radial inflow rotor turbine consists of two parts: The working wheel and the exducer wheel. The rotor consists of 15 full blades with radial-flow inlet and axial-flow outlet. The rotor flowpath is presented in Figure 5 where the radial blades at the inducer inlet are visible. The trailing-edge, the leading-edge thickness and the rotor axial, tip and radial clearance are constant whereas the blockage factor is 0.98.

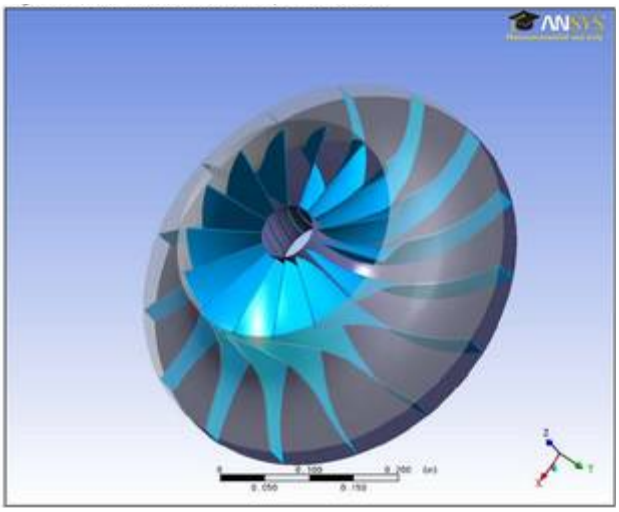

FIGURE 5. ROTOR BLADE CONFIGURATION.

Table 3 presents the rotor geometric and thermodynamic output parameters at the design point calculate by OFC.

TABLE 3. ROTOR AEROTHERMODYNAMIC OUTPUTS.

Description	Inlet ($_2$) Values	Outlet ($_3$) Values		Units
Blade height	33.51	99.67		mm
Radius	227.94	**Shroud ($_{3s}$)**	131.06	mm
		Hub ($_{3h}$)	31.39	
Axial length	125.15	--		mm
Thickness	1	1		mm
Number of blades	15			--
Relative flow angle	-25	**Shroud ($_{3s}$)**	-22.52	◦
		Hub ($_{3h}$)	-60	
Absolute flow angle	77.50	0		◦
Ratio of rotor exit shroud to inlet diam.	0.57	--		--
Ratio of rotor exit hub to inlet diam.	0.13	--		--
Ratio of rotor exit hub to shroud diam.	--	0.23		--
Tip clearance	1	1		mm
Total temperature	1123	812.66		K
Static temperature	975.45	793.09		K
Total pressure	373.19	108.90		kPa
Static pressure	227.94	100		kPa
Absolute velocity	544.42	200.68		m/s
Blade speed	586.468	**Shroud ($_{3s}$)**	83.24	m/s
		Hub ($_{3h}$)	347.58	
Relative velocity	130.01	**Shroud ($_{3s}$)**	217.26	m/s
		Hub ($_{3h}$)	401.36	

The obtained main geometrical sizes of the radial-inflow turbine using the presented design method are well agreed with that of the reference validated design [8].

MEANLINE AND PERFORMANCE DESIGN BASED ON COMPONENT CORRELATIONS.

This section covers performance analysis of the nozzle and radial-inflow rotor for a 600 kW cycle gas turbine engine using a one-dimensional computer FORTRAN code. The basic design parameters and flow characteristics of radial-inflow turbine for a 600 kW designed using the presented aerothermodynamic method are given in reference [8]. Design point performance is covered first, defining load operation at inlet conditions and the performance projection is accomplished using customized models for gas turbine cycle analysis. The predicting off-design is covered second. The predicted performance is given for a 455.88 mm diameter radial-inflow turbine. The approach is straightforward, incorporating fundamental thermodynamic relations with gas properties determined as local functions of composition and temperature.

Table 4 describes the design input aerothermodynamics parameters used in the CFD simulation. The performance analyses were conducted in air at nominal turbine inlet condition [8].

TABLE 4. BASIC DESIGN PARAMETERS OF THE RADIAL-INFLOW TURBINE FOR A 600 kW MICROTURBINE.

Design parameters	Values	Units
P_{00}	396.0	kPa
T_{00}	1123	K
$\dot{m}$	4.5	Kg/s
N_{ss}	25148.71	rpm
P_3	100	kPa

The overall performance of the turbine was evaluated in terms of efficiencies, turbine pressure ratio and the tip speed/spouting velocity ratio. Table 5 describes the non-dimensional performance parameters at the off-design point calculate by OFC.

TABLE 5. NON-DIMENSIONAL PERFORMANCE PARAMETERS.

$\eta_{ts} = \frac{1-(T_{02}/T_{01})}{1-(P_2/P_{01})^{\frac{k-1}{k}}}$	2)	Total to static efficiency
$\eta_{tt} = \frac{1-(T_{02}/T_{01})}{1-(P_{02}/P_{01})^{\frac{k-1}{k}}}$	3)	Total to total efficiency
$\eta_{tt} = \frac{1-(P_{02}/P_{01})^{\eta_p\left(\frac{k-1}{k}\right)}}{1-(P_{02}/P_{01})^{\left(\frac{k-1}{k}\right)}}$	4)	Polytropic efficiency
$\frac{U_2}{C_{OD}} = \sqrt{\left(\frac{k-1}{2}\right)\left(\frac{(U_2/a_{00})^2}{1-(P_3/P_{00})^{\frac{k-1}{k}}}\right)}$	5)	Tip speed/spouting velocity ratio
$\frac{C_{m3}}{U_2} = \left(\frac{D_{3m}}{D_2}\right)\cot\beta_{3m}$	6)	Axial exit flow coefficient
$\frac{b_2}{D_2} = \frac{\dot{m}}{2\pi\rho_2 C_{m2} r_2^2}$	7)	Ratio of nozzle vane height to rotor inlet diameter
$\frac{\dot{m}\sqrt{T_{02}}}{P_{02}}$	8)	Mass flow parameter

Table 6 describes the non-dimensional output performance parameters at the design and off-design point calculate by OFC.

TABLE 6. NON-DIMENSIONAL OUTPUT PERFORMANCE PARAMETERS CALCULATED BY OFC.

Description	Symbol	Value
Reaction	D_{rt}	0.59
Specific speed	N_{ss}	0.56
Specific diameter	D_s	3.27
Axial exit flow coefficient	C_{m3}/U_2	0.36
Total to total efficiency calculated by OFC	η_{tsc}	76.06
Total to total efficiency	η_{tt}	82.83
Radius ratio of the rotor	r_{3s}/r_2	0.63
Ratio of nozzle vane height to rotor inlet diameter	b_2/D_2	0.08
Diameter ratio	D_{3m}/D_2	0.39
Nozzle-rotor interspace	r_1/r_2	1.04
Nozzle-rotor interspace [9]	$(r_1/r_2)_W$	1.33

RADIAL-INFLOW TURBINE GEOMETRY.

Turbine geometry was examined in detail for calculated points and near the curve of maximum static efficiency. Several design parameters were then plotted as functions of specific speed to illustrate the changes in optimum turbine shape. The geometrical size of the designed nozzle and the radial-inflow rotor turbine are show in Figure 6.

$$N_{ss} = \frac{60(2g)^{3/4}}{\sqrt{\pi}} \left(\frac{\dot{w}}{\dot{w}_s}\right)^{3/4} \left(\frac{U_2}{C_2}\right)^{3/2} \left(\frac{C_3}{U_3}\right)^{1/2} \left(\frac{D_{3m}}{D_2}\right)^{3/2} \left(\frac{b_2}{D_{3m}}\right)^{1/2} \quad 9)$$

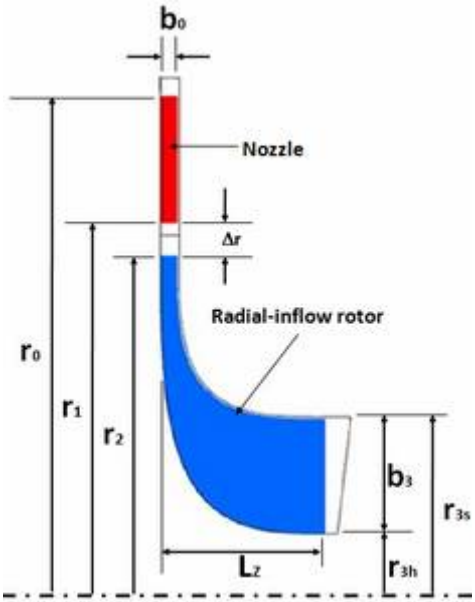

FIGURE 6. RADIAL-INFLOW TURBINE IN MERIDIONAL VIEW.

Evaluating the nozzle design.

The number of studies of nozzle performance which have been published are too limited to enable authoritative conclusions to be drawn about nozzle modelling and design, and only indications of appropriate values are available.

The nozzle vane aerodynamics loading is also direct function of the number of vanes. Figure 7 presents the variation of nozzle exit absolute flow angle (α_1) as function of the specific speed. A continuous decrease from α_1 = 83° to 52° occurs as specific speed increases from 0.2 to 1.34. For the design point (PP), α_1 = 77.93 this value is 3.76% above the value obtained by reference [6].

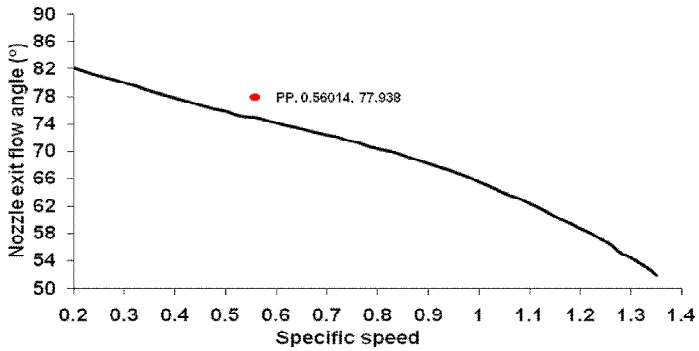

FIGURE 7. VARIATION IN NOZZLE EXIT FLOW ANGLE CORRESPONDING TO MAXIMUM STATIC EFFICIENCY WITH SPECIFIC SPEED [10].

Figure 8 shows the minimum number of nozzle vanes (Z_{bb}) as function of nozzle exit absolute flow angle for different values of nozzle inlet absolute flow angle (α_0), nozzle vane radius ratios (r_0/r_1) and ideal nozzle efficiency (η_n = 100%). The ideal or hypothetic design point (PP_{id}) for the ideal nozzle efficiency (η_n = 100%), is positioned below the nozzle vane radius ratio curve from 1.2 and between nozzle inlet absolute flow angle curves range from 55° to 50°.

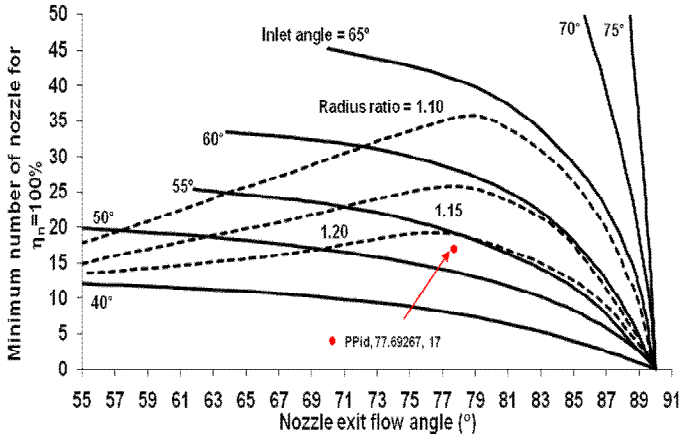

FIGURE 8. PREDICTED CORRELATION OF MINIMUM NOZZLE VANE NUMBER WITH VANE INLET AND EXIT ANGLES AND VANE INLET/EXIT RADIUS RATIO [6].

Other considerations are:

Limitations on the radial-inflow nozzle are similar to those for an axial-flow nozzle: exit vane angle should be less than 75° ($\alpha_1 < 75°$ for a radial-inflow nozzle, this is measured from the

radial direction) and trailing-edge thickness should be 0.38 mm or greater. For the design point (PP), α_1 = 77.93 this value is 3.76% above the value obtained by reference [11].

Reference [12] recommends using a nozzle vane radius ratios in the range from 1.2 to 1.3, while reference [13] advises that this value should be in the range from 1.1 to 1.7. The value used was r_0/r_1 = 1.2 and it is also shown in Figure 8.

Finally, for the nozzle-rotor interface (Δr), reference [9] recommends values less than 1.33; reference [11] recommend values below 1.05 or less and reference [6] suggests a minimum value of 1.04. The value obtained by OFC was Δr = 1.04 is within the limits recommended by the authors, and 21.76% below the maximum recommended value ($\Delta r \leq 1.33$).

Evaluating the radial-inflow rotor.

Once the basic stage design specifications are available, the important rotor sizing can be accomplished. The literature provides some useful guidelines for evaluating the rotor sizing results.

Figure 9 shows the variation in total to total efficiency (η_{tt}) as function of specific speed for a selection of nozzle exit flow angles. For each value of (α_1) a hatched area is drawn, inside of which the various diameter ratios are varied. The envelope of maximum (η_{tt}) is bounded by the constraints for $N_{ss} \geq 0.58$ in these hatched regions. This envelope is the optimum geometry curve and has a peak (η_{tt}) of 0.87 at N_{ss} = 0.58. For the design point (PP), α_1 = 77.93 this value is 5.70% above the value obtained by [10].

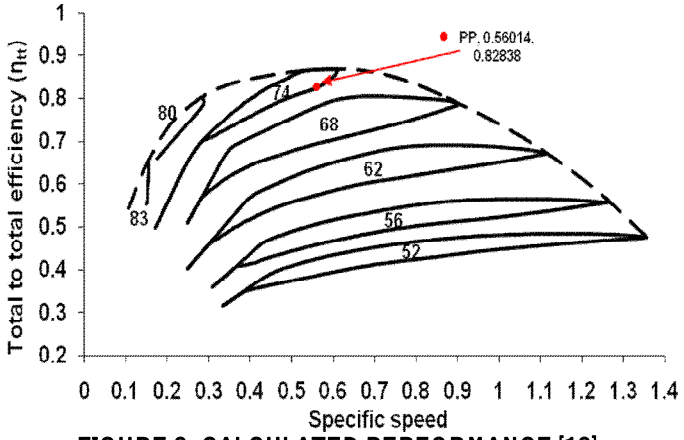

FIGURE 9. CALCULATED PERFORMANCE [10].

Figure 10 shows the variation of the blade tip speed/spouting velocity ratio, (U_2/C_{OD}) as function of axial exit flow coefficient, (C_{m3}/U_2) for different values of total to static efficiency (η_{ts}). From this figure it can be seen that peak efficiency values are obtained with velocity ratios close to 0.7 and with values of exit flow coefficient between 0.2 and 0.3. The design point (PP) is positioned below the total to static efficiency curve from 78% this value is 2% above the value obtained by reference [10].

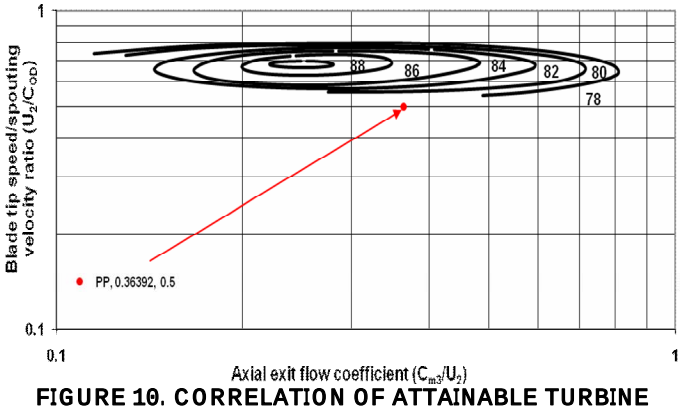

FIGURE 10. CORRELATION OF ATTAINABLE TURBINE EFFICIENCY AGAINST VELOCITY RATIOS [14].

Figure 11 shows the variation of total to total efficiency as function of polytropic efficiency (η_p) for different values of radial-inflow rotor total to total pressure ratio (RP_{ttr}). For the design point (PP), RP_{ttr} = 3.45 this value is positioned below the radial-inflow rotor total to total pressure ratio from 4.

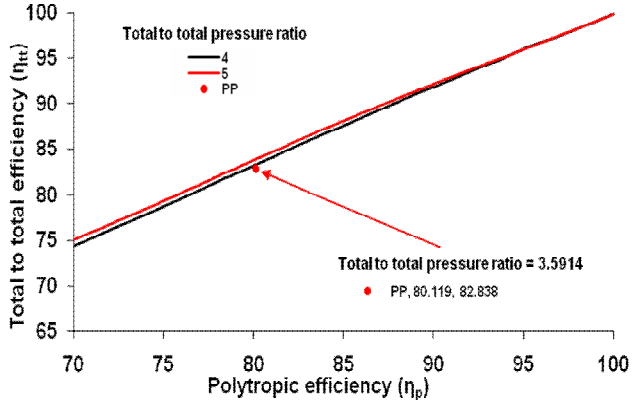

FIGURE 11. RELATIONSHIP BETWEEN POLYTROPIC AND ISENTROPIC EFFICIENCY DURING THE EXPANSION [15].

Figure 12 shows the ratio of nozzle vane height to rotor inlet diameter (b_2/D_2) increases from 0.012 to peak of 0.159 as specific speed increases. This trend is in agreement with that of nozzle exit angle and reflects the increase in nozzle flow area that accompanies the increase in volume flow and specific speed.

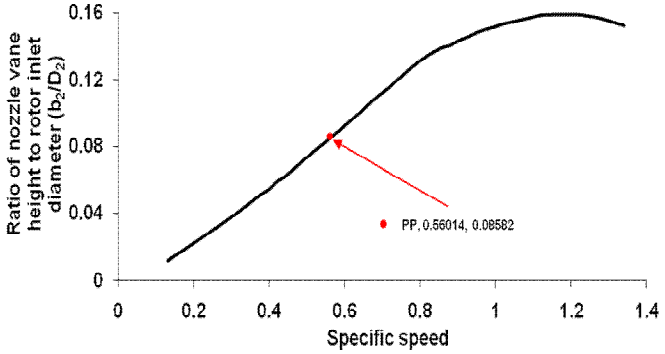

FIGURE 12. EFFECT OF SPECIFIC SPEED ON NOZZLE VANE HEIGHT FOR MAXIMUM EFFICIENCY [10].

OFF-DESIGN CHARACTERISTICS.

Characterization of turbomachinery performance at off-design conditions is through component performance maps, as would typically be generated in the course of the design cycle using dedicated turbomachinery analysis software [16].

Figure 13 presents the mass flow parameter ($\dot{m}\sqrt{T_{02}} / P_{02}$) plotted against total to static pressure ratio (P_{00} / P_3) for lines of constant speed. The design point (PP) was 3.80 and at each speed the mass flow increases with total to static pressure ratio until it reaches a maximum when the turbine is to be in choked and further increases in total to static pressure ratio do not result in any greater mass flow rate. All of the curves in Fig. 13 collapse into a single curve occur in narrow band of total to static pressure ratio 5 to 6.5 due the nozzle chokes first, the choked mass flow rate is not a function of the rotational speed because the nozzle do not rotate [17].

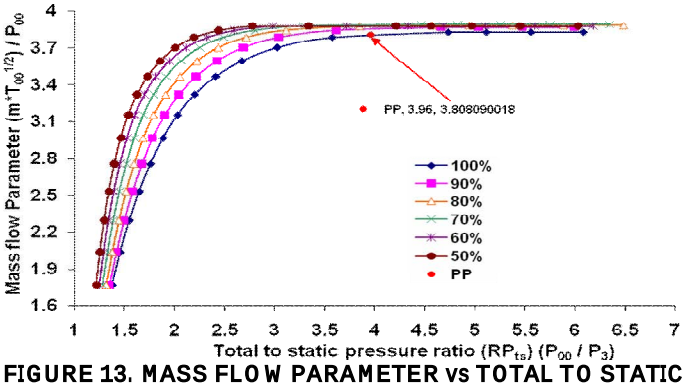

FIGURE 13. MASS FLOW PARAMETER vs TOTAL TO STATIC PRESSURE RATIO [17].

Figure 14 shows the total to static efficiency plotted against total to static pressure ratio for lines of constant speed. The maximum efficiency occurs in quite narrow band of total to static pressure ratio 2.5 to 3.5, particularly at speeds below the design point (rotational speed = 90%) [17].

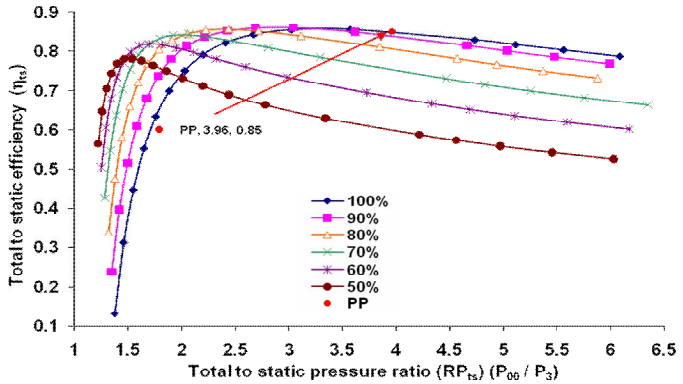

FIGURE 14. TOTAL TO STATIC EFFICIENCY vs TOTAL TO STATIC PRESSURE RATIO [17].

Figure 15 presents the total to static efficiency over the range of turbine velocity ratio (U_2/C_{OD}) investigated for lines of constant blade speed. The figure shows that a static efficiency of 85% and the velocity ratio U_2/C_{OD} = 0.66 were obtained at equivalent design point operation. This value is lower than of the ideal value (U_2/C_{OD} = 0.7) of 4.9% [17].

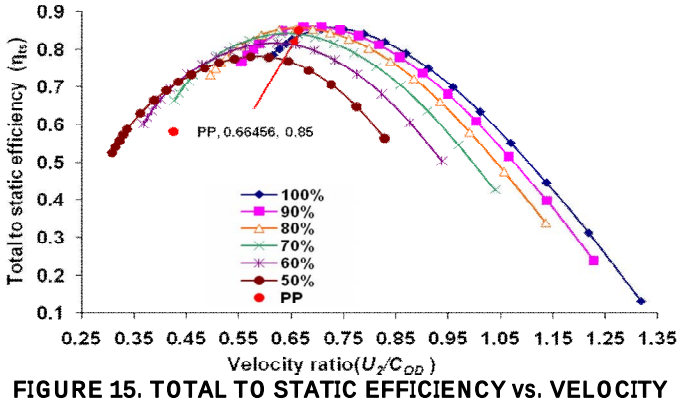

FIGURE 15. TOTAL TO STATIC EFFICIENCY vs. VELOCITY RATIO [17].

Figure 16 presents the mass flow parameters as a function of total to static pressure ratio for a nominal rotational speed, generated by CFD and OFC for the design point. The both programs have the same behavior in quite narrow band of pressure ratio 2.3 to 4.7 and the mass flow parameter obtained by OFC was 3.80. This value is 1.14% lower than of the value obtained by CFD [17].

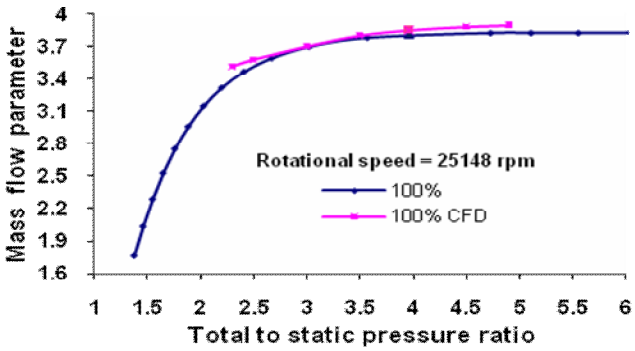

FIGURE 16. MASS FLOW PARAMETER BY CFD AND COMPARISON WITH OFC [17].

Finally, Figure 17 presents the total to static efficiency as function of total to static pressure ratio at the nominal rotational speed, generated by CFD and OFC for the design point. The both programs have the same behavior in quite narrow band of pressure ratio 3.0 to 4.8 [17].

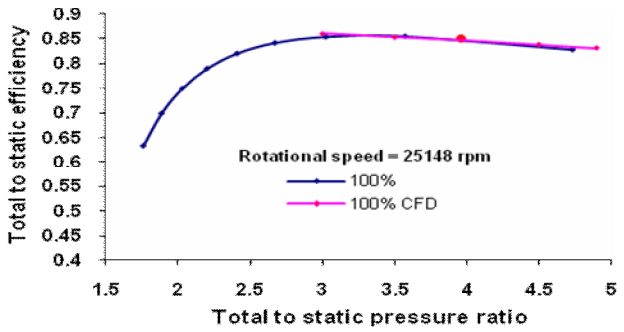

FIGURE 17. TOTAL TO STATIC EFFICIENCY BY CFD AND COMPARISON WITH [17].

CONCLUSIONS.

The main conclusions are:

- The OFC used in the design of radial turbine components is an effective route to preliminary design and optimization. The meanline model was tested and capable of providing the designer with reliable performance estimates.
- The importance of the nozzle and rotor throat areas in the prediction of choked flow is highlighted, and this in turn requires estimation of the throat blockage in addition to the geometric flow areas.
- The overall computed results from the program of this paper show a marked improvement over those from the previously used program and good agreement with analytical data.
- The main contribution of this work is that it provides a one-dimensional computer FORTRAN code (OFC) method that helps designers to quantify the performance of the nozzle and the radial inflow rotor turbine at a preliminary design stage.

ACKNOWLEDGEMENTS.

The authors wish to thank the Petrobras Research and Development Center (CENPES), the Coordination of Improvement of Higher Education (CAPES), the National Council of Technological and Scientific Development (CNPq), and the Foundation for Research Support of Minas Gerais (FAPEMIG) for their collaboration and support in the development of this work.

REFERENCES.

[1] McLallin, K. and Haas, J., (1980), "Experimental performance and analysis of 15.04-centimeter-tip-diameter, radial-inflow turbine work factor of 1.126 and thick blading", NASA TP -1730, Report N° E-391, Lewis Research Center, National Aeronautics and Space Administration, Cleveland, Ohio, USA, 20 p.

[2] Deng, Q., Niu, J., Mao, J. and Feng, Z., (2007), "Experimental and numerical investigation on overall performance of a radial inflow turbine for 100 kW microturbine", ASME TURBOEXPO 2007, Montreal, ASME GT2007-27707.

[3] Compaq Computer Corporation. Compaq Visual Fortran. 2000.

[4] Baines, N.C., (2005), "Radial turbines: An integrated design approach", Concepts NREC, Concepts ETI, Inc.

[5] Qiu, X., and Baines, N., (2007), "Performance prediction for high pressure-ratio radial inflow turbines", ASME TURBOEXPO 2007, Montreal, ASME GT2007-27057.

[6] Moustapha, H., Zelesky, M., Baines, N. C. and Japikse, D., (2003), "Axial and radial turbines", Concepts NREC, Vermont, USA, 358 p.

[7] Glassman, A.J., (1976), **"**Computer program for design analysis of radial-inflow turbines", NASA TN D-8164, Report N° E-8394, Lewis Research Center, National Aeronautics and Space Administration, Cleveland, Ohio, USA, 64 p.

[8] Miranda, R. A., Nascimento, M.A.R., Gutiérrez, E. and Moura, N., (2010), "Radial inflow turbine one and tri-dimensional design analysis of 600 kW simple cycle gas turbine engine", ASME TURBOEXPO 2010, Glasgow, ASME GT2010-22951.

[9] Watanabe, I., Ariga, I. and Mashimo, T., (1970), "Effect of Dimensional Parameters of Impellers on Performance Characteristics of a Radial-Inflow Turbine", Paper N° 70-GT-90, ASME, New York.

[10] Rohlik, H. E., (1968), "Analytical Determination of Radial Inflow Turbine Design Geometry for Maximum Efficiency", NASA TN D-4384. Report N° E-3996, Lewis Research Center, National Aeronautics and Space Administration, Cleveland, Ohio, USA, 36 p.

[11] Logan, E. and Ramentra, R., (1995), "Handbook of Turbomachinery", Second Edition, Marcel Dekker, NY, U.S.A., 185 p.

[12] Kofskey, M. G. and Nusbaum, W. J., (1972), "Effects of Specific Speed on Experimental Performance of a Radial-Inflow Turbine", NASA TN D-6605, National Aeronautics and Space Administration, Washington, DC, USA.

[13] Aungier, R. H., (2006), "Turbine Aerodynamics: Axial-Flow and Radial-Inflow Turbine Design and Analysis", ASME PRESS, New York, USA, 394 p.

[14] Dixon, B. S. L., (1998), "Fluid Mechanics and Thermodynamics of Turbomachinery", Fourth Edition, Butterworth-Heinemann, UK, 321 p.

[15] Boyce, M., (2006), "Gas Turbine Engineering Handbook", Third Edition, Houston - Texas, Gulf Professional, 955 p.

[16] Wasserbauer, C. A. and Glassman, A. J., (1975), "FORTRAN Program for Predicting the Off-Design Performance of Radial Inflow Turbines", NASA TN-8063. Report N° E-8368, Lewis Research Center, National Aeronautics and Space Administration, Cleveland, Ohio, USA, 57 p.

[17] MIRANDA, R. A. C. (2010), Design and Performance Analysis of Radial Inflow Turbine, Itajubá, 224p. MSc. Dissertation - Instituto de Engenharia Mecânica, Universidade Federal de Itajubá.

